

RSC Advances



This is an *Accepted Manuscript*, which has been through the Royal Society of Chemistry peer review process and has been accepted for publication.

Accepted Manuscripts are published online shortly after acceptance, before technical editing, formatting and proof reading. Using this free service, authors can make their results available to the community, in citable form, before we publish the edited article. This *Accepted Manuscript* will be replaced by the edited, formatted and paginated article as soon as this is available.

You can find more information about *Accepted Manuscripts* in the [Information for Authors](#).

Please note that technical editing may introduce minor changes to the text and/or graphics, which may alter content. The journal's standard [Terms & Conditions](#) and the [Ethical guidelines](#) still apply. In no event shall the Royal Society of Chemistry be held responsible for any errors or omissions in this *Accepted Manuscript* or any consequences arising from the use of any information it contains.

Cite this: DOI: 10.1039/c0xx00000x

www.rsc.org/xxxxxx

COMMUNICATION

Inflammatory modulation of stem cells by Magnetic Resonance Imaging (MRI)-detectable nanoparticles

Sezin Aday^{a,b,#}, Jose Paiva^{a,b,#}, Susana Sousa^b, Renata S.M. Gomes^c, Susana Pedreiro^d, Po-Wah So^e, Carolyn Ann Carr^f, Lowri Cochlin^g, Ana Catarina Gomes^b, Artur Paiva^d, and Lino Ferreira^{a,b,*}

Received (in XXX, XXX) Xth XXXXXXXXXX 20XX, Accepted Xth XXXXXXXXXX 20XX

DOI: 10.1039/b000000x

In the current work, we labelled human hematopoietic stem cells with polymeric nanoparticles (NPs) that can be tracked by Magnetic Resonance Imaging (MRI) and studied their effect on cell metabolism, proliferation, secretomics, genomics and differentiation. We showed that NPs had no effect on the stem cell differentiation program but affected their paracrine activity.

Hematopoietic stem cells (HSCs) are being evaluated in several clinical trials for the treatment of the heart after angina¹ or infarction², chronic wounds^{3,4}, ischemic limb^{5,6}, etc... MRI is the most attractive imaging modality to track cells because it provides high-quality 3-dimensional functional and anatomic information with high contrast⁷. Emulsions containing fluorine are being used to label different type of cells since there is no fluorine in the human body, and therefore cells labeled with these NPs can be selectively imaged by ¹⁹F MRI⁸⁻¹⁰. Unfortunately, so far it is unclear the effect of the NPs in the biology of stem cells, particularly in their differentiation program as well as their paracrine activity. Studies have shown that superparamagnetic iron NPs coated with protamine sulfate had no measurable cytotoxicity on HSCs but their effect in the differentiation and paracrine activity of HSCs was not demonstrated¹¹. In addition, self-assembling ferumoxytol-heparin protamine nanocomplexes were also used as labeling agents for MRI¹². The internalization of these nanocomplexes by HSCs (1.33 ± 0.2 pg iron/cell) slightly decreased the proliferation of HSCs and proliferative capacity of the cells was recovered only after 30 days.

Here we studied the effect of poly(lactic acid-co-glycolic acid) (PLGA) NPs containing perfluoro-1,5-crown ether (PFCE) with an average diameter of 210 nm (therefore named as NP210-PFCE) and polydispersity index of 0.12 ± 0.01 (Fig. 1A), that have the capacity to track cells¹³, on the viability, proliferation, secretomics, genomics and differentiation of hematopoietic stem/progenitor cells (CD34⁺ cells). Endothelial cells (ECs) have been used as control. Initially, internalization studies were performed using fluorescence activated cell sorting (FACS) and fluorimetry to calculate the percentage of the cells labeled and the amount of NPs internalized by the cells, respectively. Cytotoxicity profile of the NP210-PFCE formulation was evaluated by cell counting, ATP production, LDH release, ROS production, secretion of pro-inflammatory cytokines and gene expression. Then, the effect of NP formulation on the differentiation capacity of CD34⁺ HSCs was evaluated. Finally, the mechanism underlying the anti-inflammatory effect of our NPs was studied. Our results show that NPs have no substantial effect in cell proliferation, metabolism and differentiation of CD34⁺ cells or ECs; however, the NPs significantly reduced the

inflammatory activity of CD34⁺ cells but not ECs, as evaluated by gene microarray and protein secretion analysis.

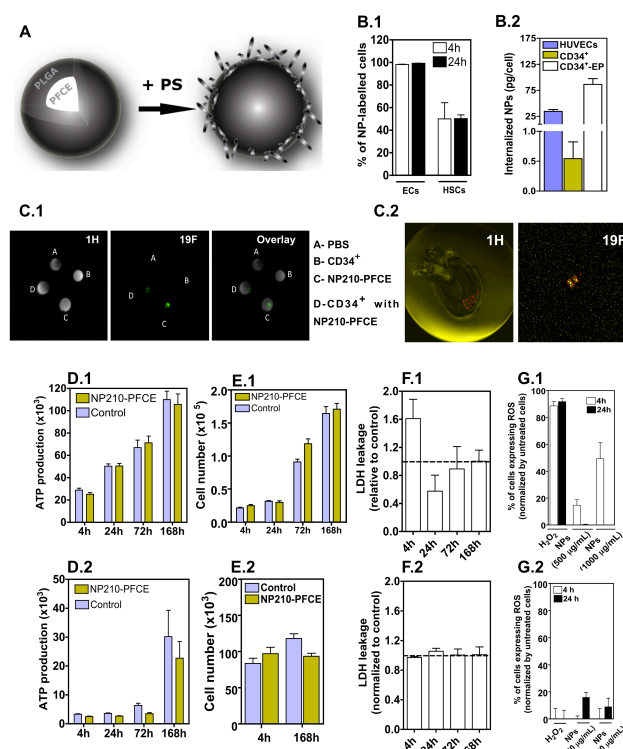


Fig. 1 Cell tracking, internalization and cytotoxicity of the NPs. (A) Schematic presentation of the NP composition. The NPs are formed by PLGA encapsulating PFCE. The NP is then coated with PS, to facilitate cell internalization. (B.1) Percentage of HUVECs or CD34⁺ cells labeled with fluorescence NPs as assessed by flow cytometry, immediately after 4 h incubation or followed by 20 h of culture in the absence of NPs (total time: 24 h). (B.2) Amount of NPs internalized by HUVECs and CD34⁺ cells as assessed by fluorimetry (EP corresponds to electroporated cells). In B.1 and B.2, results are average \pm SEM, $n=3$. (C) ¹⁹F MRI of CD34⁺ cells labeled with NPs after electroporation. (C.1) MR images of eppendorfs containing unlabeled cells (7.5×10^6 cells), cells transfected with NP210-PFCE (7.5×10^6 cells), NP210-PFCE (10 mg) and PBS. CD34⁺ cells were transfected with 2 mg/mL of NPs for 24 h. (C.2) MR images of 10 million CD34⁺ cells labeled with NPs (transfection for 4 h, 0.5 mg/mL) and injected into the myocardium of Sprague Dawley (SD) rats after ligation of the left anterior descending coronary artery (LAD) to create myocardial infarction. (D) ATP production of unlabeled and NP-labeled HUVECs (D.1) or CD34⁺ cells (D.2). Results are average \pm SEM, $n=4$. (E) Cell proliferation of unlabeled or NP-labeled HUVECs (E.1) or

CD34⁺ cells (E.2). Results are average \pm SEM, $n=4$. (F) Leakage of the lactate dehydrogenase (LDH) from NP-labeled HUVECs (F.1) or CD34⁺ cells (F.2) relatively to unlabeled cells. Results are average \pm SEM, $n=4$. (G) Percentage of HUVECs (G.1) or CD34⁺ cells (G.2) expressing ROS. Untreated cells and hydrogen peroxide (H₂O₂)-treated cells were used as negative and positive controls, respectively. Results are average \pm SEM, $n=3$. In B, D, E, F, G cells were incubated with the NPs for 4 h and then washed to remove NPs that were not internalized by the cells.

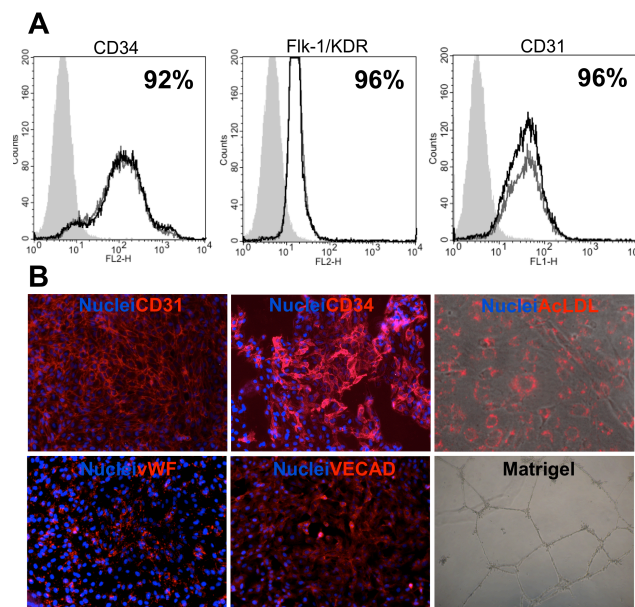


Fig. 2 Impact of NPs on the endothelial differentiation program of CD34⁺ cells. (A) Flow cytometric analysis of vascular markers (CD31, CD34 and Flk-1/KDR) on ECs derived from unlabelled (dark grey) and NP-labelled CD34⁺ cells (black). Percent of positive cells were calculated based in the isotype controls (grey plot) and are shown in the histogram plots. (B) Characterization of ECs derived from NP-labelled CD34⁺ cells by immunofluorescence and functionality. ECs express CD31, CD34, vWF, and vascular endothelial-cadherin (VE-CAD). ECs metabolize Ac-LDL and form microvessels on top of Matrigel.

Next, we investigated the impact of the NPs on both cells by gene microarray analysis. Gene expression in HUVECs was not statistically significant in cells treated or not with NPs. In contrast, CD34⁺ cells showed more than 100 genes that were statistically ($p<0.001$) significant and grouped in 5 categories and 15 sub-categories (Fig. 3A). Interestingly, the most affected cellular function was immune response, being 41 genes downregulated at 24 h, and 7 genes at day 7 (Supplementary Tables 2-8). In addition, there was an increase in the expression of the genes that prevent oxidative stress, in particular metallothioneins (MTs)¹⁵.

Some of the genes identified in the microarray analysis have been confirmed by qRT-PCR (Fig. 3B). The cellular expression of MTs at mRNA level is dependent on the initial concentration of the NPs that cells were exposed to (Fig. 3C). Importantly, the anti-inflammatory properties of NP210-PFCE are not shared by superparamagnetic iron oxide NPs (SPION), very often used in MRI applications, which have a similar internalization level (0.27 ± 0.01 pg/cell) as NP210-PFCE (Fig. 3B). To confirm the impact of the NPs, we evaluated the secretion of pro-inflammatory cytokines in cells exposed to NPs for 24 h by Bioplex. CD34⁺ cells incubated with NPs show a decrease in the secretion of pro-inflammatory cytokines (e.g. IFN- γ , IL-8, MCP-1, MIP-1 β , TNF- α) (Fig. 3D). In contrast, HUVECs containing NPs increased the secretion of IL-6 (~2.0 fold) and MCP-1 (~1.5 fold) among all cytokines tested (Fig. 3E). Altogether, our results show that the exquisite properties (chemistry (PLGA, PS or PFCE), size or geometry) of NP210-PFCE are unique in inducing the anti-inflammatory properties on CD34⁺ cells. Further testing is needed to elucidate this issue. Although not shown, soluble protamine sulfate has no anti-inflammatory properties on CD34⁺ cells.

NP210-PFCE containing 176.5 μ g of PFCE per mg of PLGA was coated with protamine sulfate (PS; approximately 13 μ g of PS per mg of NP), a cationic agent to facilitate intracellular delivery (Fig. 1A)¹¹. In these conditions, NP210-PFCE had an average diameter of 210 nm and a zeta potential of 7.0 ± 1.7 mV. HUVECs and CD34⁺ cells were exposed to fluorescent-labeled NPs (500 μ g/mL) for 4 h, harvested and labeling efficiency of the cells was assessed by Fluorescence Activated Cell Sorting (FACS) and fluorimetry. FACS results show that 95% (ECs) and 50% (CD34⁺) of the cells were labeled after 4 h (Fig. 1B.1). Fluorescence measurements indicate that this labeling corresponds to the internalization of 34.7 ± 3.4 and 0.5 ± 0.3 pg of PFCE per cell of HUVECs and CD34⁺, respectively (Fig. 1B.2). When the CD34⁺ cells were electroporated and incubated with higher concentrations (2 mg/mL) of NPs up to 24 h, the internalized amount of NPs increased up to 86.4 ± 11.2 pg of PFCE per cell *in vitro* (Fig. 1B.2). Under this loading condition, which is comparable to fluorine-based liposomes used in the literature for different cell types⁸, the cells can be tracked by MRI (Fig. 1C.1) However, MRI can also monitor CD34⁺ cells *in vivo* without electroporation (Fig. 1C.2).

NP210-PFCE internalized by CD34⁺ cells or ECs have no substantial effect in cell proliferation, metabolism and oxidative stress. Cells labeled with fluorescent NPs were sorted by flow cytometry before evaluation. Both cells transfected with NP210-PFCE show similar cell metabolism, as assessed by an ATP assay, and cell proliferation as compared to untreated cells (Figs. 1D and 1E). In addition, after 24 h, no significant differences were observed in LDH release on CD34⁺ cells or HUVECs treated with or without NPs, showing that NPs do not significantly affect cell membrane integrity (Fig. 1F). Moreover, CD34⁺ cells cultured with NPs show low capacity to generate ROS even after 24 h of culture (Fig. 1G). The relative low effect of NPs in ROS generation is likely due to CD34⁺ cell capacity to tolerate oxidative stress due to high expression and activity of antioxidant enzymes (see below)¹⁴. This phenomenon might explain the toleration of the cells to NPs and H₂O₂. ECs cultured for 4 h in the presence of NP210-PFCE generate ROS but then the levels drop off to baseline levels if cells were cultured for additional 20 h in the absence of NPs. Together, our results indicate that the oxidative stress induced by NPs was moderate in CD34⁺ cells and ECs and the increase in ROS was time-, dose- and cell-dependent.

NP210-PFCE formulation has no effect on the endothelial differentiation capacity of CD34⁺ cells. CD34⁺ cells transfected with NP210-PFCE for 4 h were then sorted to isolate the ones containing NPs. Both untreated and NP-treated CD34⁺ cells attached to the culture dish after 15-20 days of culture with a cobblestone-like morphology and expressed high levels of EC markers⁴ (Fig. 2). No differences were observed in terms of kinetics or phenotype between both cells. Overall, our results indicate that NP210-PFCE has no measurable effect in the *in vitro* differentiation program of CD34⁺ cells.

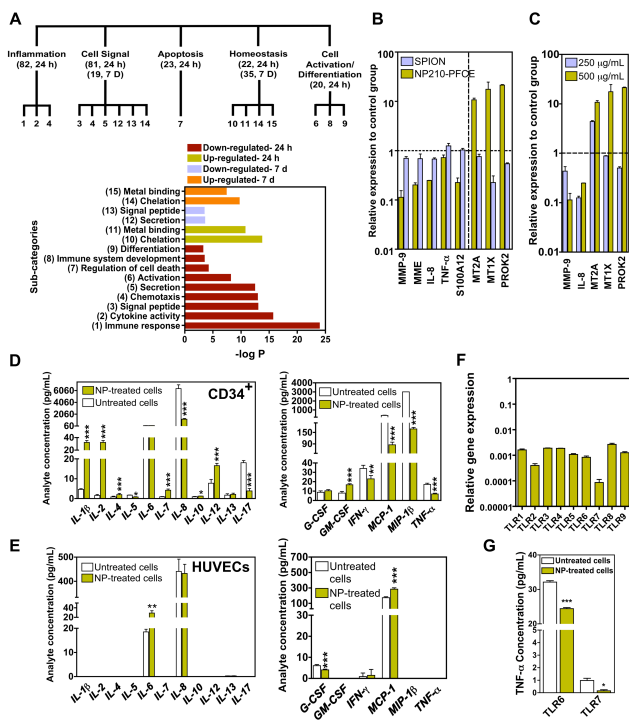


Fig. 3 Effect of NPs in gene expression and secretion of chemokines/cytokines by CD34⁺ cells. (A) Classification of genes into functionally related gene groups. Functional categories (inflammation, apoptosis, cell activation/differentiation, cell signal and homeostasis) and sub-categories significantly affected in CD34⁺ cells labeled with NPs. The number of genes affected at different time points is given inside parentheses. $-\log P$ values for different sub-categories for 24 h and 7 d are given in a column bar graph. (B-C) Validation of gene expression by qRT-PCR after 24 h. The dashed line represents the separation of down-regulated and up-regulated genes. Control group corresponds to the cells without NPs after 24 h. Results are average \pm SEM, $n=4$. In C, gene expression was evaluated in CD34⁺ cells exposed to different concentrations of NP210-PFCE. (D-E) Secretome analysis. Seventeen cytokines were measured simultaneously in medium collected from unlabeled or NP-labeled HUVECs (E) or CD34⁺ cells (D). Cells were exposed to the NPs for 4 h. Results are Mean \pm SEM ($n=3$). (F) Expression of toll-like receptors (TLR 1-9) in CD34⁺ cells after isolation from human cord blood. Results are Mean \pm SEM ($n=3$). (G) Secretion of TNF- α by unlabeled and NP-labeled CD34⁺ cells when activated by FSL1 (TLR6) and imiquimod (TLR7). Results are Mean \pm SEM ($n=3$). In D, E and G, *, **, *** denotes statistical significance ($p<0.05$, $p<0.01$, $p<0.001$, respectively).

NP210-PFCE formulation interferes with agonist-mediated activation of TLRs. TLRs are pattern-recognition receptors that allow cells to recognize and protect tissues from various harmful stimuli¹⁶. At least 10 human TLRs have been identified so far, being TLRs 1, 2, 4, 5 and 6 mainly located on the cell surface while TLRs 3, 7, 8 and 9 mostly found in the endocytic compartments¹⁷. Cellular activation of TLRs leads to the expression of inflammatory cytokines and chemokines. CD34⁺ cells express 9 TLRs at mRNA level, being TLR2 and TLR7 the lowest expressed (Fig. 3F). Next, we evaluated whether CD34⁺ cells labeled with NP210-PFCE showed attenuated activation of agonist-mediated activation of TLRs. From all the TLRs tested, the activation of TLR6 and TLR7 by TLR agonists was significantly decreased ($P<0.001$ for TLR6 and $P<0.05$ for TLR7) (Fig. 3G). Overall, our results indicate that the immunomodulatory properties of the NP210-PFCE are mediated by TLR6 and TLR7.

Conclusions

This work shows that NPs with the capacity to track stem cells may have immunomodulatory properties. Previous studies have used several NP formulations to track CD34⁺ cells *in vivo* (e.g. superparamagnetic¹⁸ as well as nanocomplexes¹²) by MRI; however, the effects of NPs in stem cell biology were never addressed using high-throughput characterization techniques such as gene arrays. Our results show that NPs may interfere with CD34⁺ TLRs attenuating their secretion of inflammatory cytokines. Although studies have shown that NPs (specifically silver NPs) can inhibit the secretion of pro-inflammatory cytokines (IL-6, IL-8, TNF- α , etc...) on macrophages mediated by specific TLRs¹⁹, such studies were never extended to HSCs and more specifically to NPs with the capacity to track stem cells. The immunomodulatory properties of NPs may be relevant in a biomedical context since it has been shown that inhibition of TLR and proinflammatory cytokine signaling contributes critically to ischemic tolerance in different organs^{20, 21}. Injured tissue and necrotic cells release endogenous activators (TLR ligands)²², which activate TLRs and causes of high level of inflammatory cytokine secretion and cellular injury. However, down-regulation of proinflammatory TLR and cytokine signaling reduces the acute inflammatory response that worsens ischemic injury. Different studies showed that both TLR2- and TLR4-deficient mice show less injury upon cerebral ischemia²³. Similarly, our NPs might be an interesting tool to increase ischemic tolerance and cell survival in different organs. Altogether, the NPs described in this work represent a novel class of NPs for MRI imaging while acting as an anti-inflammatory agent.

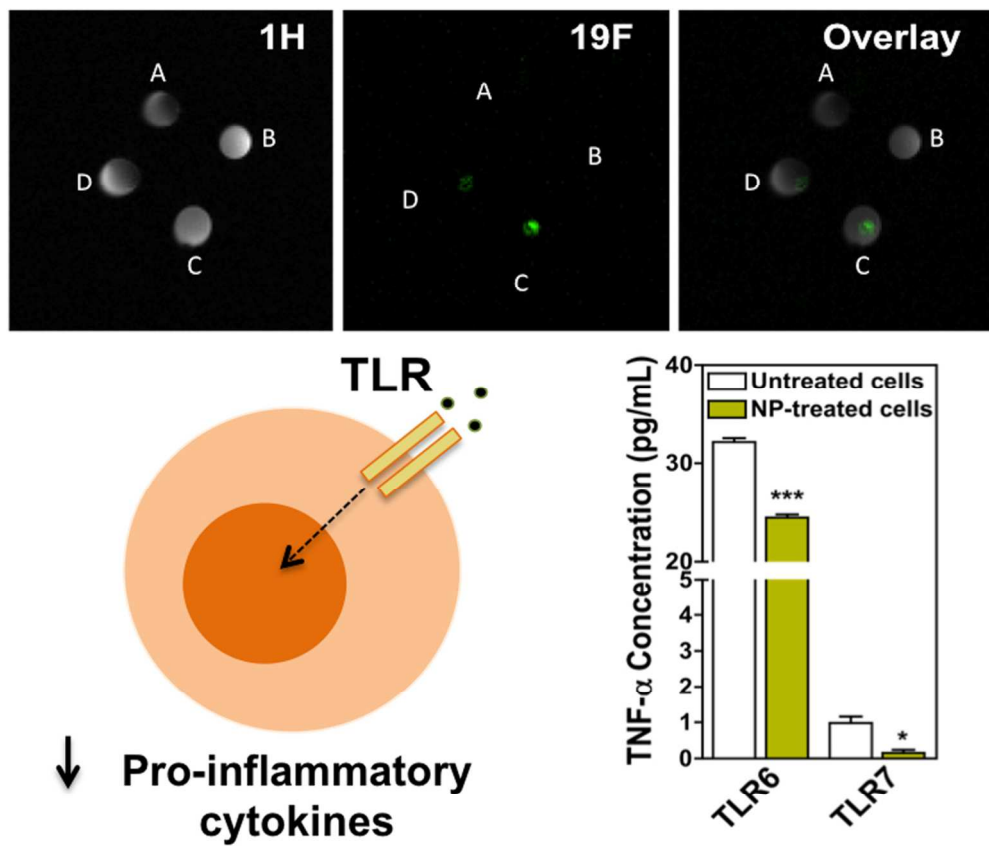
Acknowledgements

This work was supported by a Marie Curie-Reintegration Grant (FP7-People-2007-4-3-IRG; contract n° 230929), MIT-Portugal program, FCT (PTDC/CTM/099659/2008; and SFRH/BD/42871/2008, a fellowship to S.A.) and COMPETE funding (Project "Stem cell based platforms for Regenerative and Therapeutic Medicine", Centro-07-ST24-FEDER-002008).

Notes and references

- ^a CNC-Center for Neurosciences and Cell Biology, University of Coimbra, Coimbra, Portugal.
- ^b Biocant, Biotechnology Innovation Center, Cantanhede, Portugal.
- ^c King's BHF Centre of Excellence, Cardiovascular Proteomics, King's College London, London, UK.
- ^d Centro de Histocompatibilidade do Centro, Coimbra, Portugal.
- ^e Department of Neuroimaging, Institute of Psychiatry, King's College London, London, UK.
- ^f Cardiac Metabolism Research Group, Department of Physiology, Anatomy & Genetics, University of Oxford, UK.
- ^g PulseTeq Limited, Chobham, Surrey, UK.
- ⁹⁰ † Electronic Supplementary Information (ESI) available: Details on experimental methods and supplementary tables. See DOI: 10.1039/b000000x/
- [#] These authors contributed equally to this work.
- 95 1. D. W. Losordo, R. A. Schatz, C. J. White, J. E. Udelson, V. Veereshwarayya, M. Durgin, K. K. Poh, R. Weinstein, M. Kearney, M. Chaudhry, A. Burg, L. Eaton, L. Heyd, T. Thorne, L. Shturman, P. Hoffmeister, K. Story, V. Zak, D. Dowling, J. H. Traverse, R. E. Olson, J. Flanagan, D. Sodano, T. Murayama, A. Kawamoto, K. F. Kusano, J. Wollins, F.

- Welt, P. Shah, P. Soukas, T. Asahara and T. D. Henry, *Circulation*, 2007, 115, 3165-3172.
2. V. Schachinger, S. Erbs, A. Elsasser, W. Haberbosch, R. Hambrecht, H. Holschermann, J. Yu, R. Corti, D. G. Mathey, C. W. Hamm, T. Suselbeck, B. Assmus, T. Tonn, S. Dimmeler and A. M. Zeiher, *N Engl J Med*, 2006, 355, 1210-1221.
3. O. Awad, E. I. Dedkov, C. Jiao, S. Bloomer, R. J. Tomanek and G. C. Schatteman, *Arterioscler Thromb Vasc Biol*, 2006, 26, 758-764.
- 10 4. D. C. Pedroso, A. Tellechea, L. Moura, I. Fidalgo-Carvalho, J. Duarte, E. Carvalho and L. Ferreira, *PLoS One*, 2011, 6, e16114.
5. R. J. Powell, W. A. Marston, S. A. Berceli, R. Guzman, T. D. Henry, A. T. Longcore, T. P. Stern, S. Watling and R. L. Bartel, *Mol Ther*, 2012, 20, 1280-1286.
- 15 6. R. Passier, L. W. van Laake and C. L. Mummery, *Nature*, 2008, 453, 322-329.
7. A. Stroh, C. Faber, T. Neuberger, P. Lorenz, K. Sieland, P. M. Jakob, A. Webb, H. Pilgrim, R. Schober, E. E. Pohl and C. Zimmer, *Neuroimage*, 2005, 24, 635-645.
- 20 8. E. T. Ahrens, R. Flores, H. Xu and P. A. Morel, *Nat Biotechnol*, 2005, 23, 983-987.
9. M. Srinivas, P. A. Morel, L. A. Ernst, D. H. Laidlaw and E. T. Ahrens, *Magn Reson Med*, 2007, 58, 725-734.
- 25 10. Y. B. Yu, *J Drug Target*, 2006, 14, 663-669.
11. A. S. Arbab, G. T. Yocum, H. Kalish, E. K. Jordan, S. A. Anderson, A. Y. Khakoo, E. J. Read and J. A. Frank, *Blood*, 2004, 104, 1217-1223.
12. M. S. Thu, L. H. Bryant, T. Coppola, E. K. Jordan, M. D. Budde, B. K. Lewis, A. Chaudhry, J. Ren, N. R. Varma, A. S. Arbab and J. A. Frank, *Nat Med*, 2012, 18, 463-467.
- 30 13. R. S. Gomes, R. P. Neves, L. Cochlin, A. Lima, R. Carvalho, P. Korpisalo, G. Dragneva, M. Turunen, T. Liimatainen, K. Clarke, S. Yla-Herttuala, C. Carr and L. Ferreira, *ACS Nano*, 2013, 7, 3362-3372.
- 35 14. T. He, T. E. Peterson, E. L. Holmuhamedov, A. Terzic, N. M. Caplice, L. W. Oberley and Z. S. Katusic, *Arterioscler Thromb Vasc Biol*, 2004, 24, 2021-2027.
15. S. K. Baird, T. Kurz and U. T. Brunk, *Biochem J*, 2006, 394, 275-283.
- 40 16. J. Lee, J. W. Sohn, Y. Zhang, K. W. Leong, D. Pisetsky and B. A. Sullenger, *Proc Natl Acad Sci U S A*, 2011, 108, 14055-14060.
17. S. Akira, S. Uematsu and O. Takeuchi, *Cell*, 2006, 124, 783-801.
18. M. Lewin, N. Carlesso, C. H. Tung, X. W. Tang, D. Cory, D. T. Scadden and R. Weissleder, *Nat Biotechnol*, 2000, 18, 410-414.
- 45 19. P. M. Castillo, J. L. Herrera, R. Fernandez-Montesinos, C. Caro, A. P. Zaderenko, J. A. Mejias and D. Pozo, *Nanomedicine (Lond)*, 2008, 3, 627-635.
- 50 20. K. Kariko, D. Weissman and F. A. Welsh, *J Cereb Blood Flow Metab*, 2004, 24, 1288-1304.
21. Y. C. Wang, S. Lin and Q. W. Yang, *J Neuroinflammation*, 2011, 8, 134.
22. Y. Shi and K. L. Rock, *Eur J Immunol*, 2002, 32, 155-162.
- 55 23. S. C. Tang, T. V. Arumugam, X. Xu, A. Cheng, M. R. Mughal, D. G. Jo, J. D. Lathia, D. A. Siler, S. Chigurupati, X. Ouyang, T. Magnus, S. Camandola and M. P. Mattson, *Proc Natl Acad Sci U S A*, 2007, 104, 13798-13803.



Novel MRI-detectable PLGA nanoparticles can track hematopoietic stem cells and down-regulate the secretion of pro-inflammatory cytokines by interfering with TLRs.
49x45mm (600 x 600 DPI)